Design and performance of a prototype polarization modulator rotational system for use in space using a superconducting magnetic bearing

T. Matsumura, H. Kataza, S. Utsunomiya, R. Yamamoto, M. Hazumi, N. Katayama

***Abstract*—We present the design and the mechanical and thermal performances of a prototype rotational mechanism using a superconducting magnetic bearing (SMB) for a space compatible polarization modulator. The rotational mechanism consists of an SMB with an optical encoder and three grip mechanism that holds a levitating rotor until a high temperature superconducting array (YBCO) cools down below its critical temperature. After the successful operation of a grip mechanism, the rotor magnet levitates at 10-16 K and we conduct spin down measurements. We estimate the heat dissipation from the rotor rotation and an optical encoder. From the mechanical and thermal performances of the prototype rotation mechanism, we did not find the potential no-go results from this SMB technology for use in a future space mission. The development of this rotational mechanism is targeting for use of a polarization modulator for a space mission to probe the comic inflation by measuring the cosmic microwave background polarization.**

***Index Terms*—Superconducting magnetic bearing, polarization modulator, space application**

I. Introduction

The cosmic microwave background radiation (CMB) is a relic light from the big bang. It started to free stream 380,000 years after the beginning of the universe, and we can still observe them today as the 3 K black body radiation. The measurements of the CMB have provided rich information about the physics of early universe including the contents and the dynamics of the universe.

In order to explain the observed universe today, there is a theoretical hypothesis of the existence of cosmic inflation, i.e. rapid expansion of the universe just after the beginning of the universe, ~10^{-38} sec. The inflation theory predicts the presence of the CMB B-mode polarization pattern at the large angular scale if the inflation exists. Thus, the physics of such an early universe appears to be unreachable, but the inflation paradigm is testable by the measurements of the CMB polarization.

The expected signal amplitude of the inflation is about ~10^{-9} smaller than the 3 K black body radiation. Thus, any CMB polarization experiments that try to probe the inflationary B-mode need to have unprecedented precision by enough statistics and controlling the systematics.

One of the key candidate instruments that can achieve these two requirements simultaneously is to employ a polarization modulator using a half-wave plate (HWP) [1,2]. A typical experiment needs about a > 300 mm diameter of HWP that rotates continuously at a few Hz and an operating temperature of about 4 K. The experimental challenge is to achieve the continuous rotation at the cryogenic temperature without dissipating too much heat.

EBEX is one of the frontier CMB polarization experiments using the HWP based polarization modulator. It employs a rotation mechanism of the modulator by using a superconducting magnetic bearing (SMB) as a continuously rotating cryogenic bearing [3,4,5]. This instrument was developed for a balloon-borne CMB experiment, and deployed in the EBEX long duration balloon flight from Antarctica in 2012.

This HWP based polarization modulator using an SMB is now a potential candidate for a future satellite mission. Although the technological demonstration exists in a balloon-borne format, the use of any moving part based technology in a space mission adds extra challenges to be demonstrated as listed,

- low power consumption
- protect the modulator from a launch vibration
- radiation tolerance
- weight

In this paper, we describe the prototype design of the SMB based polarization modulator for a future space mission. We focus on parts of the first two bullet points and describe the mechanical and thermal performances. Finally we describe the scalability in size and discuss the path forward for use this technology in a space mission.

II. Rotation Mechanism for Polarization Modulator

A. Presumptions and Requirements

We list the design presumptions and requirements as

This work was supported by JSPS KAKENHI Grant Number 15H05441. This work was also supported in part by Strategic Fund from the Steering Committee for Space Science. *(Corresponding author: T. Matsumura.)*

T. Matsumura, H. Kataza, R. Yamamoto are from Japan Aerospace Exploration Agency (JAXA), Sagamihara, Kanagawa, Japan. (e-mail: tmatsumu@astro.isas.jaxa.jp).

S. Utsunomiya is with Japan Aerospace Exploration Agency (JAXA), Tsukuba, Japan.

M. Hazumi is with the High Energy Accelerator Research Organization (KEK).

N. Katayama and M. Hazumi are with the University of Tokyo, Kavli IPMU.

H. Kataza is also with Department of Astronomy at University of Tokyo.

R. Yamamoto is also with Department of Physics at University of Tokyo.

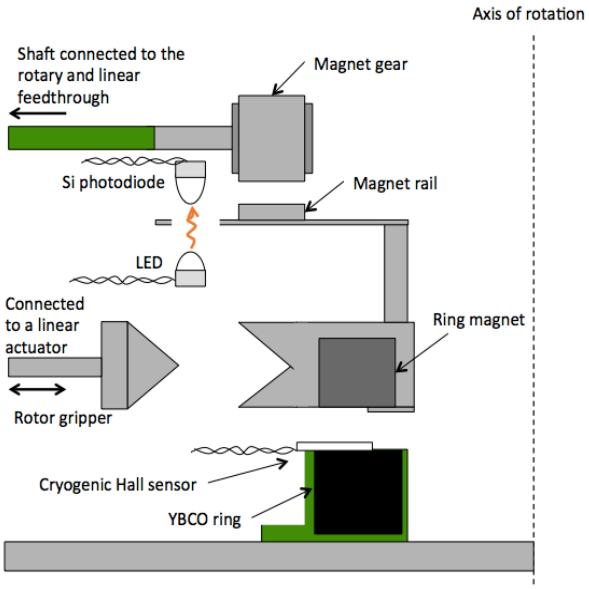

Fig. 1 The schematic cross-sectional view of the prototype rotation mechanism.

1. a modulator is cooled to about 4 K using a mechanical cooler and we allocate the total allowable cooling power of this modulator system at an operating mode to be less than 3 mW.
2. a rotor has to be held rigidly at room temperature during a launch under the launch vibration and be able to rotate once it reaches to the operating temperature at about 4 K.
3. a position angle of a rotor has to be encoded with an accuracy of 0.01 degrees.
4. a prototype design has to be scalable to an opening diameter of 420 mm for use in a forthcoming application, such as the next generation CMB polarization satellite, LiteBIRD [6].

B. Prototype design

Fig. 1 shows the prototype rotational mechanism for the HWP based continuously rotating polarization modulator. We employ the SMB for the supporting bearing. The rotor is a NdFeB permanent magnet, PM, ring with remnance of 1.1 Tesla. The stator is a high temperature superconductor, HTS, array (YBCO) [7]. The size of the PM and HTS rings are listed in Table 1**.** The levitation height is set at 5 mm.

The three holder arms with cryogenic stepping motors serve as a mechanism to hold the rotor in place above the critical temperature of the HTS [8]. Fig. 2 shows the overview of the hardware including the three stepping motors. Fig. 3 shows the grip mechanism. This also serves as a launch lock during the rocket launch.

An optical encoder consists of an LED and silicon photodiode. The LED emits in the infrared (wavelength of 850 nm). The LED and silicon photodiode are placed face-to-face between an optical chopper. The chopper has 60 opening holes with arc-shaped slots (three-degree opening angle).

A cryogenic Hall sensor is mounted just under the rotor magnet. This serves partly as an encoder using the variation of the rotor magnetic field non-uniformity and partly as a levitation monitor.

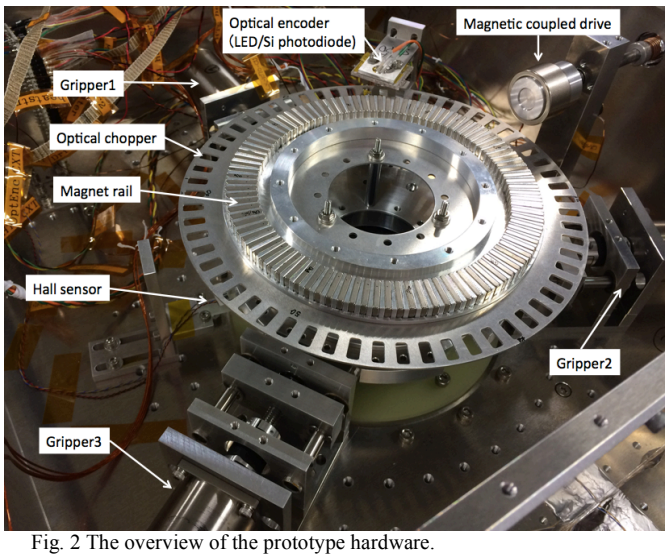

Fig. 2 The overview of the prototype hardware.

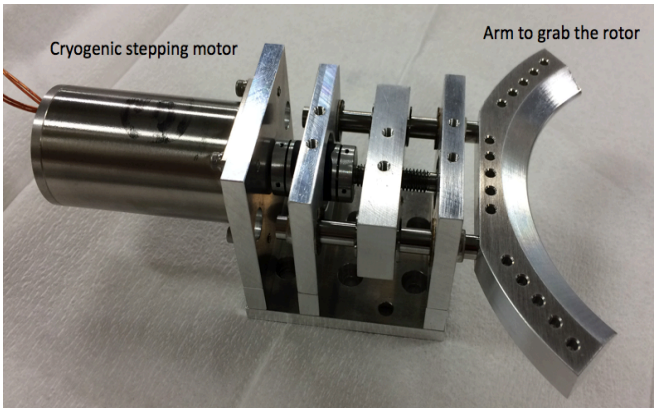

Fig. 3 The grip mechanism.

The rotation is initiated by using a magnetic coupled gear. The drive shaft with a magnetic coupler drives the magnetic rail that is mounted on the second floor of the rotor magnet.

Table 1 The size of the rotor magnet and the HTS stator.

	Material	ID [mm]	OD [mm]	H [mm]
PM	NdFeB	65	85	12
HTS	YBCO	55	95	18

III. Experiments

We conducted spin down measurements in two configurations.
Configuration 1: We place the experimental setup (Fig. 2) in a Styrofoam box. We submerge it with liquid nitrogen (LN2) up to the height of the HTS array. Thus, the rotor is free to rotate under the room pressure.
Configuration 2: We place the experimental setup in a cryostat that is mechanically cooled by a GM cooler. The HTS and surrounding components are cooled down to about 10-16 K. A G10 hollow drive shaft is connected from the outside of the cryostat through a linear and rotational feedthrough. This magnetic gear provides the initial kick for spin down measurements.

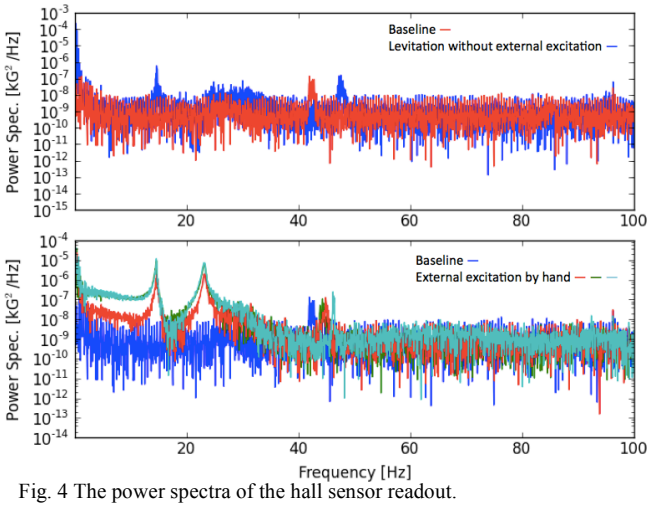

Fig. 4 The power spectra of the hall sensor readout.

In both configurations, we measured the spin down rate using the optical encoder. We also used the Hall sensor to measure the resonance frequency. Furthermore, we measured the optical encoder signal shape as a function of a current bias to the LED.

IV. Results

A. Coefficient of friction

Table 2 shows the spin down results for two configurations. We fit the spin down results with a model,

$$\alpha = 2\pi \frac{df}{dt} = a_0 + 2\pi a_1 f, \qquad (1)$$

where α is the coefficient of friction, t is time, f is the rotational frequency, and a_0 and a_1 are fit parameters. The fitted values are summarized in Table 1. Using the moment of inertia of the rotor we can estimate the heat dissipation assuming the energy loss during the spin down converts to a heat. The derived heat dissipations at the rotational frequency at 1 Hz are also in Table 2.

Table 2 The fit results and the derived heat dissipation due to the friction.

	a_0 [1/s^2]	a_1 [1/s]	P [μ W]
LN2 at room pressure	-1.6×10^{-3}	-1.6×10^{-3}	73
Cryostat	-1.3×10^{-3}	-2.2×10^{-4}	19

Note: The cryostat row corresponds to the HTS temperature of 10-16 K and the pressure of less than 10^{-4} torr.

B. Resonance frequency

Fig. 4 shows the power spectrum of the Hall sensor readout

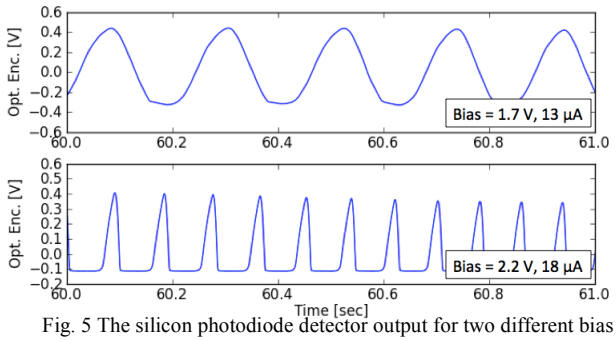

Fig. 5 The silicon photodiode detector output for two different bias currents.

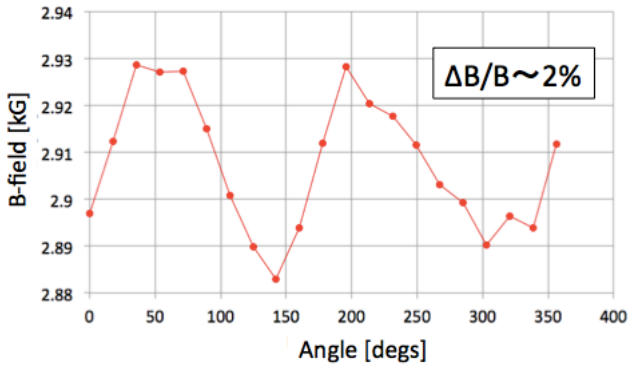

Fig. 6 The axial magnetic field as a function of the circumference of the prototype magnet.

in Configuration 1. We identified the resonance peaks at 14.5 and 23.5 Hz for the horizontal and vertical oscillation modes, respectively. We also observed an unidentified resonance frequency at around 45 Hz. This feature exists when the rotor is not levitating, and thus we conclude that this feature is not related to the vibrational mode of the levitating rotor.

C. Heat dissipation from the optical encoder

Fig. 5 shows the optical encoder signal with two bias currents at 10 K. Both examples show sufficiently high signal-to-noise. The difference comes due to the non-linear response of the photodiode in the encoder. The maximum power dissipation for the case in the bottom panel corresponds to 40 μ W.

V. Discussions

We discuss the heat dissipation of the larger diameter SMB system for use in a space mission. During the continuous rotating operation, the dominant heat source is the coefficient of friction of the rotor. While the heat dissipation is 19 μ W in the Configuration 2 test, the size of the rotor has to be bigger than the one in the prototype. We scale the power dissipation to the 420 mm opening diameter rotor via the moment of inertia, I, as

$$P = I\alpha = \frac{1}{2} M(R_i)(R_i^2 + R_o^2), \qquad (2)$$

where M is the mass of the ring shape rotor. The mass scales linearly with the inner diameter R_i, and the outer diameter is $R_o = R_i + dR$, and dR is the width of the ring. We assumed that the height and width of the rotor ring is kept the same. Therefore, the moment of inertia of the ring shaped magnet scales about the third power of the inner radius of the rotor ring. The corresponding expected heat dissipation is 5.2 mW.

We discuss the several potential for the improvements. One is to minimize the source of eddy current loss, i.e. minimize the a_1 term contribution in Equation (1). If the a_1 term is negligible, the expected heat dissipation is 2.8 mW. The majority of the material of the current prototype is made of aluminum, including the surrounding structure of the rotating PM. This can be replaced by the non-metallic material and/or implement the slots to minimize the current path, and thus minimize the eddy current loss.

The other possibility for the lower heat dissipation is the

higher critical current, J_c, of YBCO. The energy loss due to the hysteresis is expected to be proportional to J_c^{-3}. The measurements in Configuration 2 is done at the HTS temperature of 10-16 K, and therefore the loss may be expected to decrease by cooling the HTS array to the lower temperature around 4 K.

The above two possibilities assume the same rotor magnet non-uniformity and extrapolates the thermal performance for a larger diameter rotor magnet. Another possibility is to minimize the axial non-uniformity of the rotor magnetic field. Figure 6 shows the non-uniformity of the rotor magnet. The magnetic field in the axial direction is measured along the circunference of the magnet. The non-uniformity, $\Delta B/B$, that is defined as the maximum difference over the mean is about 2 %. According to the Bean's model, the hystresis loss is proportional to $(\Delta B/B)^3$. One possibility may be simply to construct the rotor magnet that has lower non-uniformity, and thus less time varying magnetic field. Another parameter is the levitation height. The current levitation height, i.e. the separation distance between the surface of the HTS and the surface of the rotor magnet, is set at 5 mm. Therefore, we can increase this height to minimize the amplitude of the magnetic field non-uniformity at the HTS. The caveat is the loss of the stiffness in the levitating rotor. For use in space, there is no gravity. Thus, this optimization is purely driven by the requirement of the optical performance of the polarization modulator. Though there is a room for the optimization, addressing this issue is beyond the scope of this paper and leave it for a future study.

VI. Conclusions

We designed, constructed, and tested the prototype rotational mechanism for a space compatible polarization modulator. After the successful operation of the grip mechanism, the rotor magnet levitates and we conducted the spin down measurements. We estimate the heat dissipation from the rotor rotation and the optical encoder. We have not found the potential no-go results from this SMB technology for use in a future space mission.

Acknowledgment

T. Matsumura would like to thank to Prof. Mitsuda for the support and Dr. K. Sakai for useful discussions. This work was supported by JSPS KAKENHI Grant Number 15H05441, MEXT KAKENHI Grant Number 15H05891, and the ISAS strategic development fund from the steering committee for space science.

References

[1] T. Matsumura, "A Cosmic Microwave Background Radiation Polarimeter Using Superconducting Magnetic Bearings", Ph.D thesis at University of Minnesota, Twin Cities, 2006.

[2] A. Kusaka et al., "Modulation of CMB polarization with a warm rapidly-rotating half-wave plate on the Atacama B-Mode Search (ABS) instrument", Rev. Sci. Instrum., 85,

[3] S. Hanany et al., "A Cosmic Microwave Background Radiation Polarimeter Using Superconducting Bearings", IEEE-Transactions of Applied Superconductivity, 2003, Vol. 13.

[4] J. Klein et al., "A cryogenic half-wave plate polarimeter using a superconducting magnetic bearing", Cryogenic Optical Systems and Instruments XIII; San Diego, CA; United States; 24 August 2011 through 25 August 2011.

[5] M. Miryala, Chap. 9 of "Superconductivity: Recent Developments and New Production Technologies", Materials Science and Technologies Superconductivity Research and Applications, ISBN: 978-1-62257-137-6.2012.

[6] T. Matsumura et al., "Mission design of LiteBIRD". J. Low Temp. Phys. 176:733-740 (2014).

[7] ATZ, http://atz-gmbh.com

[8] Phytron, http://www.phytron-elektronik.de